COMPDYN 2023
9th ECCOMAS Thematic Conference on
Computational Methods in Structural Dynamics and Earthquake Engineering
M. Papadrakakis, M. Fragiadakis (eds.)
Athens, Greece, 12-–14 June 2023

ROCKING RESPONSE AND VULNERABILITY OF THE PULPIT BY GIOVANNI PISANO IN PISTOIA (ITALY)

Gianni Bartoli[1], Michele Betti[1], Luca Facchini[1] and Silvia Monchetti[1]

[1]Dept. of Civil and Environmental Engineering
University of Florence
Via S. Marta 3, 50139 Florence, Italy
e-mail: gianni.bartoli, michele.betti, luca.facchini, silvia.monchetti@unifi.it

Abstract. *The pulpit of Giovanni Pisano lies in the church of S. Andrea in Pistoia, Italy, and is one of the most outstanding marble artifacts of the late middle ages in Italy. It is composed by seven columns supporting a platform.*

The columns have different lengths, since they rest on pedestals located at different heights, in a way for the column tops to be at the same height and therefore form a support for the arches, which in turn support the platform above.

All the components are linked to each other by means of thin layers of lead; as a consequence, such connections cannot resist traction and the whole artifact is likely to exhibit rocking behavior, especially during earthquakes.

This paper describes the development of a ®MatLab code and its utilization to take into account the rocking response of the pulpit. The model has been identified making use of the dynamic recordings performed by a permanent monitoring system composed of 6 *accelerometers mounted at the base of the pulpit itself and on its platform. The first natural frequencies have been used to determine the compressibility of the lead layers.*

Subsequently, some artificial earthquakes were numerically generated to obtain an estimation of the fragility curves of the artifact, and eventually an estimation of its seismic vulnerability.

Keywords: Rocking, Nonlinear Systems, Seismic Vulnerability, Protection of Artifacts.

1 INTRODUCTION

The pulpit in the church of S. Andrea, Pistoia, is one of the most outstanding marble artifacts of the late middle ages in Italy ([1]). It was sculpted in 1301 by Giovanni Pisano, who built the entire structure on a hexagonal basis. It is sustained by six red Carrara marble columns located at each vertex of the hexagon, together with another column in the geometrical center of the pulpit itself.

The interface between the columns bottom and the ir basement, as well as between the columns top and the pulpit itself, is filled with lead and therefore cannot undergo any traction.

Little is known about its history, nevertheless it is known that in 1619 it was dismantled and reassembled in the middle of the nave, where it stands nowadays, as it can be seen in figure 1. On that occasion, the order of the marble panels which constitute the parapet was inverted.

Figure 1: on the left side, the pulpit as it is nowadays; on the right side, a snapshot of the instruments during the dynamic tests.

The artifact is subject to several critical issues and it was restored several times. In particular, the marble supporting columns are not perfectly vertical and this can be perceived even by the naked eye. As some Authors have already outlined, the causes of instability of the pulpit can be ascribed to:

- errors made in the reassemblement in the year 1619;
- differences in the characteristics of the ground on the east and the west side;
- subsidence phenomena taking place in the city center;
- sudden, impulsive or transient events such as earthquakes and similar.

It is certainly difficult to ascribe the instability to only one of the above-cited causes; rather, such instability is likely due to more than one phenomena.

2 Brief summary of the dynamic tests

The experimental campaign took place in February, 2020; ambient vibration measurements were carried out and, eventually, also some tests on each column under impulsive loads given by light blows of an instrumented hammer on the church floor nearby.

Accelerometers were placed on top and at mid-height of the marble columns; during the ambient vibration tests, the sensors were placed both on top and at mid-height of the columns according to the pattern shown in figure 2.

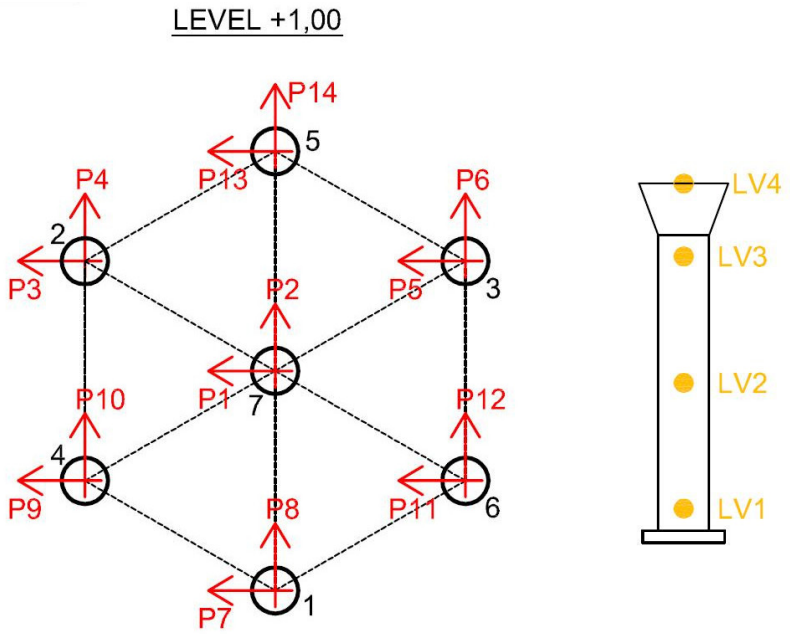

Figure 2: on the left, the arrangement of the accelerometers at column mid-height (level $1.00\,\mathrm{m}$; on the right, the position of the accelerometers on each column during the impulsive tests.)

The identified frequencies are listed in the following table; referring to figure 2 the instruments identified by odd numbers were parallel to $x-x$ direction and the instruments with even numbers in the $y-y$ direction.

modal shape	identified frequency
$x-x$	$\nu_1 = 5.11\,\mathrm{Hz}$
$y-y$	$\nu_2 = 5.32\,\mathrm{Hz}$
torsional	$\nu_3 = 6.58\,\mathrm{Hz}$

Table 1: Identified frequencies.

3 The physical model

Since the pulpit rests on seven slender columns, it likely undergoes rocking motion (see f.i. [3]). Therefore, a specific ®MatLab code was developed to investigate its dynamic behavior. The main assumptions were the following:

1. even if the pulpit is made up by seven different marble plates (as shown in figure 3) and the

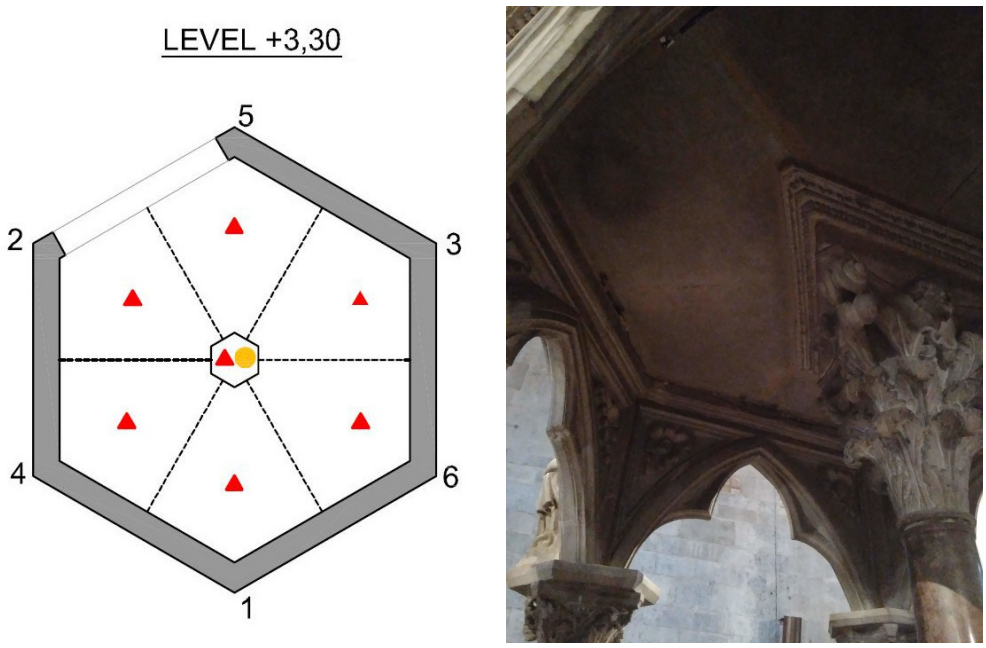

Figure 3: on the left, the seven different plates constituting the pulpit floor, at level $3.30\,\mathrm{m}$ above the church floor, are indicated by the red triangles. The shaded area indicates the parapet. On the right, a particular of the pulpit floor, seen from below, showing the connection between different plates.

panels of the parapet, which can easily break away from each other during a pronounced motion, it was assumed that the pulpit be monolithic with its parapet;

2. the internal stresses are not significant for the collapse of the pulpit; the collapse can only occur due to the overturning of the columns;

3. the vertical motion of the pulpit and the columns was neglected in the analysis;

4. the pulpit and the columns are perfectly rigid bodies and deformations can only occur inside the interface between the columns and the pulpit (above) or the basement (below);

5. such interface cannot undergo traction: therefore, the columns can uplift from their basements and the pulpit can uplift from the supporting columns, thus giving rise to non-linear behavior;

6. nevertheless, the columns cannot completely break away from neither their basements not the pulpit above, and the top of the columns always follow the motion of the pulpit;

7. the non-linearity of the structure derives by the behavior of the interfaces between the columns and the other parts of the structure; displacements are considered sufficiently small to be considered geometrically linear.

Under such hypotheses, the pulpit behaves like a rigid block resting on seven slender rigid blocks and its motion can therefore be described by only three degrees of freedom (DoFs): the displacement in two horizontal directions and the rotation around the vertical axis.

Some comments are in order about the hypotheses listed above; in particular, the first two hypotheses can be released by the definition of a critical threshold for the displacement of the top of each column; in other words, following a common strategy in the probabilistic analysis

of structural safety, the failure probability due to the internal stresses or the breaking away of the floor plates can be evaluated defining a threshold on the displacement and analyzing the first-passage time of such threshold.

The third hypothesis is the most difficult to justify, and in fact is almost never verified, as the vertical motion of a rocking structure can deeply affect the horizontal response and the overturning probability. This is the first model which was developed, and the hypothesis of negligible vertical motions will be released in further versions of the numerical code.

The fourth hypothesis is not so significant: the bending of the columns due to eccentricity of axial force has little - if any - influence on the pulpit motion; it can eventually lead to the collapse of one or more columns, but this event can be also taken into consideration by the definition of a proper threshold on the pulpit displacement.

The fifth hypothesis is the motivation of the present study, while the sixth is, in a way, a direct consequence of the irrelevance of the vertical motions of the various elements (third hypothesis).

The seventh hypothesis steams from the slenderness of the columns.

3.1 Model of the kinetic energy

Hypotheses (6) and (7) enable to easily describe the motion of each column in terms of the DoFs of the pulpit above; with regard to figure 4, if $\dot{d}_1$, $\dot{d}_2$ and $\dot{d}_3$ respectively denote the velocities in the x and y directions and the angular velocity around the vertical axis of the geometric center of the pulpit floor (namely, the derivatives of the DoFs), then the displacements and velocities in the x and y directions of the top of the h-th column are given by the law of the rigid body motion:

$$\begin{cases} s_{xh} = d_1 - d_3\, y_{ph} \\ s_{yh} = d_2 + d_3\, x_{ph} \end{cases} \quad ; \quad \begin{cases} v_{xh} = \dot{d}_1 - \dot{d}_3\, y_{ph} \\ v_{yh} = \dot{d}_2 + \dot{d}_3\, x_{ph} \end{cases} \tag{1}$$

Owing to the slenderness of the columns, their diagonal can be approximated with their length and therefore the velocity of the center of mass of each column is half as much the velocity of its top, the components being $v_{xh}/2$ and $v_{yh}/2$. The angular velocity of the column is, eventually, $\omega_h = v_h/H_h$, where $v_h = \sqrt{v_{xh}^2 + v_{yh}^2}$ is the modulus of the velocity of the top of the column, and H_h its length.

Considering equations 1, the kinetic energy of the h-th column can be expressed as

$$E_{ch} = \frac{1}{2}\, m_{ph}\, v_h^2 + \frac{1}{2}\, I_{ph}\, \omega_h^2 = \frac{m_{ph}}{8} \left(\dot{d}_1^2 + \dot{d}_2^2 - 2\, \dot{d}_1\, \dot{d}_3\, y_{ph} + 2\, \dot{d}_2\, \dot{d}_3\, x_{ph} + \dot{d}_3^2\, [x_{ph}^2 + y_{ph}^2] \right) \tag{2}$$

which, in turn, leads to the definition of the mass matrix of the generic h-th column as

$$\mathbf{M}_{ph} = \frac{m_{ph}}{4} \begin{bmatrix} 1 & 0 & -y_{ph} \\ 0 & 1 & x_{ph} \\ -y_{ph} & x_{ph} & x_{ph}^2 + y_{ph}^2 \end{bmatrix} \tag{3}$$

where m_{ph} is obviously the mass of the column.

The center of mass of the pulpit is not vertically aligned with the geometric center of its floor (where the origin of the reference system lies) owing to the presence of a statue of an eagle

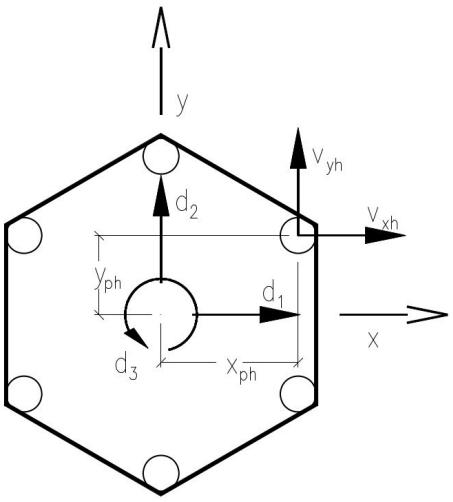

Figure 4: the relation between the DoFs of the pulpit and the velocity of the top of the h-th column.

(visible in figure 1) and to the absence of one panel of the parapet. The x and y coordinates of the center of mass of the pulpit will be denoted by x_{pg} and y_{pg}, respectively; this leads to the definition of the mass matrix of the pulpit as

$$\mathbf{M}_p = m_p \begin{bmatrix} 1 & 0 & -y_{pg} \\ 0 & 1 & x_{pg} \\ -y_{pg} & x_{pg} & i_{op}^2 + x_{pg}^2 + y_{pg}^2 \end{bmatrix} \tag{4}$$

where m_p is the mass of the pulpit and $i_{op}^2 = I_{op}/m_p$ its radius of gyration, I_{op} being the moment of inertia of the pulpit around the principal vertical axis. Since equations 3 and 4 are both referred to the same degrees of freedom, denoting by N_p the number of columns, the total mass matrix can be simply assembled as

$$\mathbf{M} = \mathbf{M}_p + \sum_{h=1}^{N_p} \mathbf{M}_{ph} \tag{5}$$

3.2 Restoring forces and moments

The interface between the columns and the pulpit (above) or their base (below) is modeled by a Winkler deformable layer with a given stiffness c_p which is assumed constant for all the 14 interfaces (2 interfaces, above and below, for each one of the 7 columns). No interface can react to traction, therefore uplift of columns from their base and of pulpit from the bearing columns is permitted, leading to strong non-linear behavior.

Referring to figure 5, it can be shown that the resultant force and moment of the pressure distribution in the interface depend on the rotation θ of the column and can be expressed (when uplift occurs) as

$$\begin{cases} R = \int_{-r}^{x_0} r_p(x)\,\mathrm{d}x \\ M = -\int_{-r}^{x_0} x\, r_p(x)\,\mathrm{d}x \end{cases} \tag{6}$$

where $r_p(x)\,\mathrm{d}x$ is the resultant force acting on an infinitesimal strip of interface, of width $\mathrm{d}x$. Therefore, it can be inferred that $r_p(x) = 2\,a(x)\,p(x)$ where $a(x) = \sqrt{r^2 - x^2}$ is half the length of the infinitesimal strip at abscissa x and $p(x) = c_p\,\theta\,(x_0 - x)$ is the upward pressure acting on such strip, r being the radius of the column base.

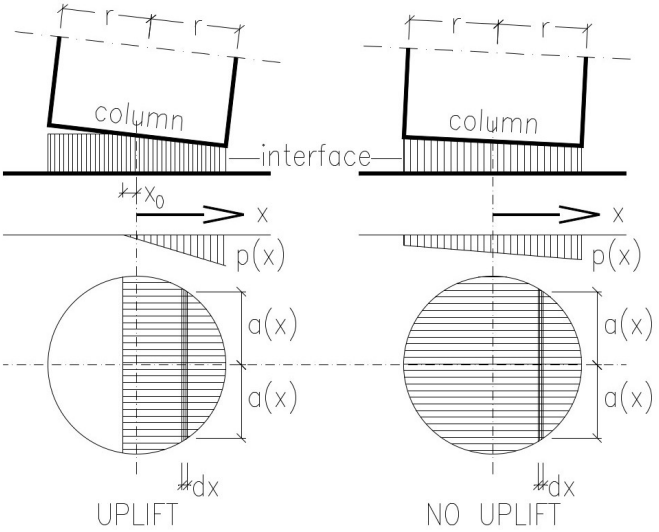

Figure 5: pressure distributions in the interface of the columns.

On the other hand, if uplift does not occur, the entire interface reacts and the resultant force and moment of the pressure distribution can be expressed as

$$\begin{cases} R = \int_{-r}^{r} r_p(x)\,\mathrm{d}x = c_p\,w_o\,A \\ M = -\int_{-r}^{r} x\,r_p(x)\,\mathrm{d}x = -c_p\,\theta\,J_y \end{cases} \tag{7}$$

where A and J_y are the area and moment of inertia of the column base, respectively, and w_o is the deflection of the interface in the center of the base. From these last equations, it follows that uplift occurs if $|w_o| < |\theta|\ r/2$.

Following and developing a previous study by Blasi and Spinelli [2], along the vertical direction the columns are subject to their own weight W_{ch}, to the part of the pulpit weight that each one bears W_{ph} and to the vertical reaction of their top and bottom sections R_{sh} and R_{ih}, respectively; for negligible vertical motion of the column center of mass, the base reaction simply balances the column weight and the part of the pulpit weight. Therefore, it is imposed that, for the h-th column,

$$\begin{cases} R_{sh} = W_{ph} & \text{on top of the column} \\ R_{ih} = W_{ch} + R_{sh} & \text{at column base} \end{cases} \tag{8}$$

The situation is described in figure 6. As a result, once W_{ch} and W_{ph} are known, the pressure distribution in the interfaces only depends on the rotation θ of each column; this leads to the calculation of the restoring moments (M_{ih} and M_{sh}) by means of equations 6.

The dependence of the moments of the pressure distribution (with respect to the geometrical centers of the top and bottom sections) acting on the top and the bottom of the column, as well as the forcing and restoring moments acting on the single column are represented in figure 6.

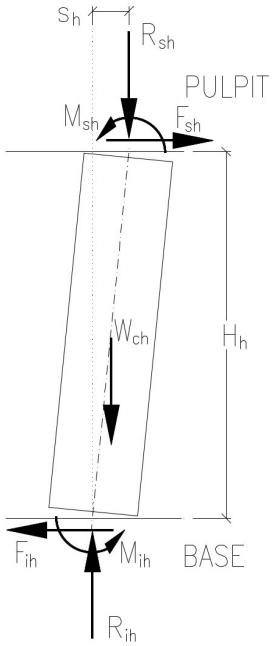

Figure 6: the forces and moments acting on the generic column.

In this framework, the system is elastic, even though non-linear. In order to determine the restoring forces on the pulpit, a static situation is considered, where the generic h-th column is rotated owing to the displacement of its top section. Considering the restoring moments acting on each column, the moment of the force F_{sh} at the top of the column must balance the moment of the column weight W_{ch} and the part of the pulpit weight W_{ph} supported by the column itself, so that

$$F_{sh} = \frac{M_{ih} + M_{sh} - R_{sh}\, s_h - W_{sh}\, s_h/2}{H_h} \tag{9}$$

The restoring moments on each column act on the pulpit as a system of restoring forces and moments which can be reduced to the DoFs of the pulpit itself, in order to construct a nonlinear stiffness matrix which depends on such DoFs, $\mathbf{K}(\mathbf{d})$. With respect to figure 8, the force $\mathbf{F}_{sh}$ applied by a column to the pulpit is opposite to the displacement of the top section of the column, $\mathbf{s}_h$, and its modulus is given by (9); if we denote by $\mathbf{w}_h$ the versor of the displacement $\mathbf{s}_h$, namely $\mathbf{w}_h = \mathbf{s}_h / \|\mathbf{s}_h\| = \mathbf{s}_h / s_h$, we obtain that

$$\mathbf{F}_{sh} = -F_{sh}\, \mathbf{w}_h = -\frac{F_{sh}}{s_h}\, \mathbf{s}_h = \frac{1}{H_h} \left(R_{sh} + \frac{W_{sh}}{2} - \frac{M_{ih} + M_{sh}}{s_h} \right) \mathbf{s}_h \tag{10}$$

Recalling equations (1), the displacement of the column top may be expressed by means of a topological matrix $\mathbf{T}^{(h)}$ defined as

$$\mathbf{T}_h = \begin{bmatrix} 1 & 0 & -y_{ph} \\ 0 & 1 & x_{ph} \end{bmatrix} \quad \Rightarrow \quad \mathbf{s}_h = \mathbf{T}_h\, \mathbf{d} \tag{11}$$

Analogously, the action of the h-th column on the pulpit can be reduced to the DoFs of the pulpit as

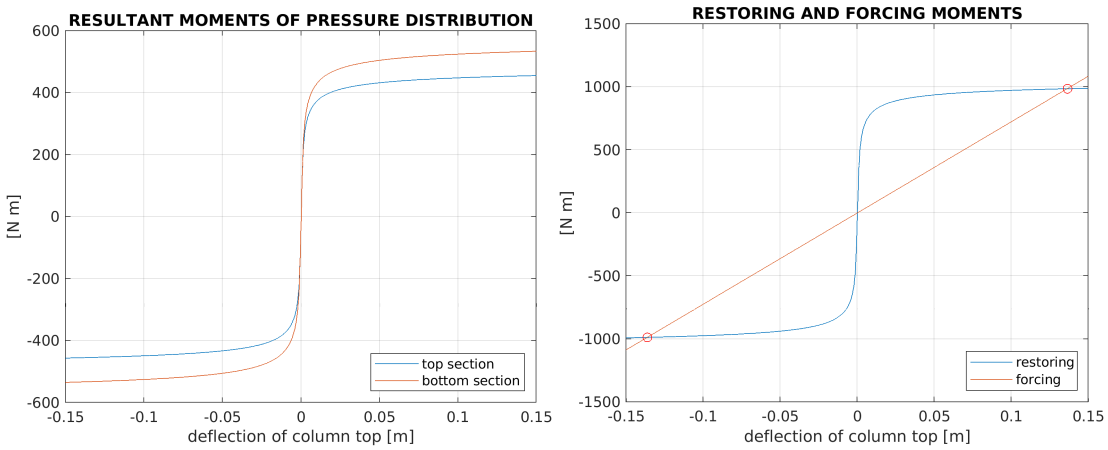

Figure 7: on the left side, the resultant moments of the pressure distribution acting on the top and bottom sections of the generic column is reported as function of the displacement of the column top (respect to its base); on the right side, the dependence of the restoring and forcing moments acting on the generic column.

$$\begin{cases} f_{1h} = F_{shx} \\ f_{2h} = F_{shy} \\ f_{3h} = -y_{ph}\, F_{shx} + x_{ph}\, F_{shy} \end{cases} \quad \Rightarrow \quad \mathbf{f}_h = \mathbf{T}_h^t\, \mathbf{F}_{sh} = \frac{R_{sh} + \frac{W_{sh}}{2} - \frac{M_{ih}+M_{sh}}{s_h}}{H_h}\, \mathbf{T}_h^t\, \mathbf{T}_h\, \mathbf{d} \tag{12}$$

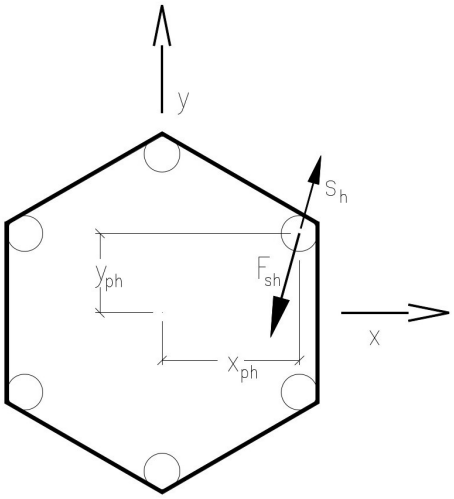

Figure 8: the restoring force caused by the generic column on the pulpit.

The non-linear stiffness matrix expressing the restoring forces on the pulpit can therefore be assembled summing all the contributions of each column:

$$\mathbf{K}(\mathbf{d}) = \sum_{h=1}^{N_p} \frac{R_{sh} + \frac{W_{sh}}{2} - \frac{M_{ih}+M_{sh}}{s_h}}{H_h}\, \mathbf{T}_h^t\, \mathbf{T}_h \tag{13}$$

The dependence of $\mathbf{K}$ on the DoFs $\mathbf{d}$ is caused by the dependence of M_{ih} and M_{sh} on $\mathbf{d}$, and is omitted for clarity.

4 Equation of motion and parameter identification

The motion of the pulpit caused by the ground motion can be described by vector $\mathbf{d}(t)$ and therefore be modeled by the vector equation

$$\mathbf{M}\,\ddot{\mathbf{d}} + \mathbf{C}\,\dot{\mathbf{d}} + \mathbf{K}(\mathbf{d})\,\mathbf{d} = -\mathbf{M}\,\mathbf{a}_g(t) \tag{14}$$

where $\mathbf{a}_g(t)$ is the ground horizontal acceleration; the components of the ground acceleration are taken according the Italian NTC 2018, namely $\pm 100\%$ of the acceleration in one direction (x or y) and $\pm 30\%$ in the other one, thus leading to 8 integrations for each couple a_{gx} and a_{gy}.

For small values of the degrees of freedom $\mathbf{d}$, the interfaces are completely reacting and the stiffness matrix $\mathbf{K}$ is constant; this allows the calculation of the modal shapes and associated frequencies of the structure.

Such frequencies obviously depend on the stiffness c_p of the interface, which is considered constant for each column; the best match between the calculated and the identified frequencies was obtained for $c_p = 2.0115 \times 10^{10}\,\mathrm{N/m^3}$, as shown in figure 9.

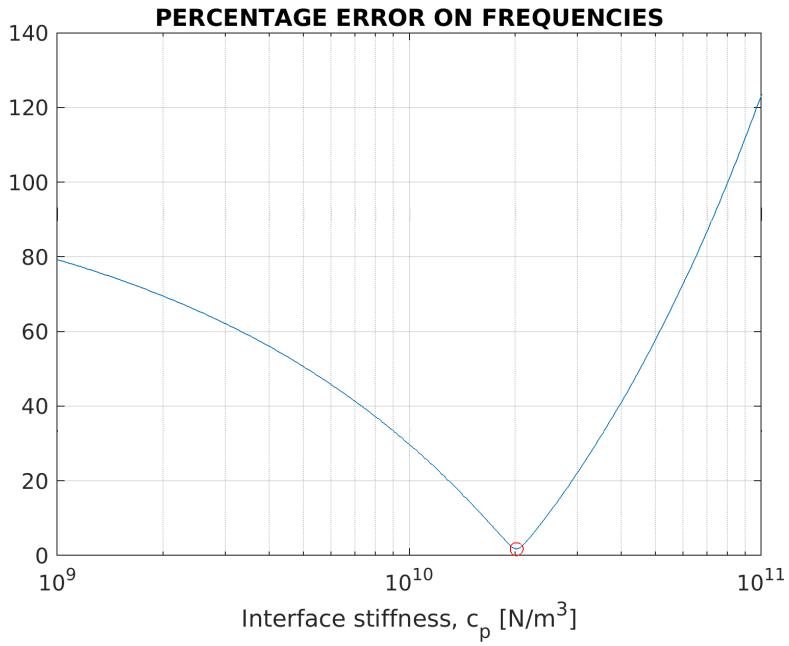

Figure 9: the percentage error obtained on the first two frequencies for various values of the interface stiffness.

The frequencies resulting for such value of the interface stiffness are listed in table 2 following, along with the frequencies identified during the dynamic tests.

modal shape	identified frequency	calculated frequency
$x - x$	$\nu_1 = 5.11\,\mathrm{Hz}$	$\nu_1 = 5.21\,\mathrm{Hz}$
$y - y$	$\nu_2 = 5.32\,\mathrm{Hz}$	$\nu_2 = 5.23\,\mathrm{Hz}$
torsional	$\nu_3 = 6.58\,\mathrm{Hz}$	$\nu_3 = 9.91\,\mathrm{Hz}$

Table 2: Identified and computed frequencies.

The error on the identified frequencies that was used to determine the stiffness of the interface was computed only on the first two frequencies, leading to a large error on the third one (the torsional one). The error can also be computed on all the three identified frequencies, but this leads to a larger error on the first two.

Damping is mainly due to different factors; one is certainly the intrinsic damping of the materials of the structure, and another one is due to impacts between the columns and their interfaces resulting from uplift. So far, damping is modeled by means of a linearly viscous model, with a modal damping matrix given by a constant modal damping $\xi = 0.05$.

5 Response statistics

A total of 100 spectrum compatible ground motions were simulated for the site of S. Andrea church in Pistoia, for different return periods T_r varying from 30 to 2475 years. In this way, for each return period, 50 couples of accelerograms were available, allowing 50 integrations of the equation of motion for each possible direction.

As an example of the obtained results, the time histories of the three degrees of freedom of the pulpit are shown in figure 10.

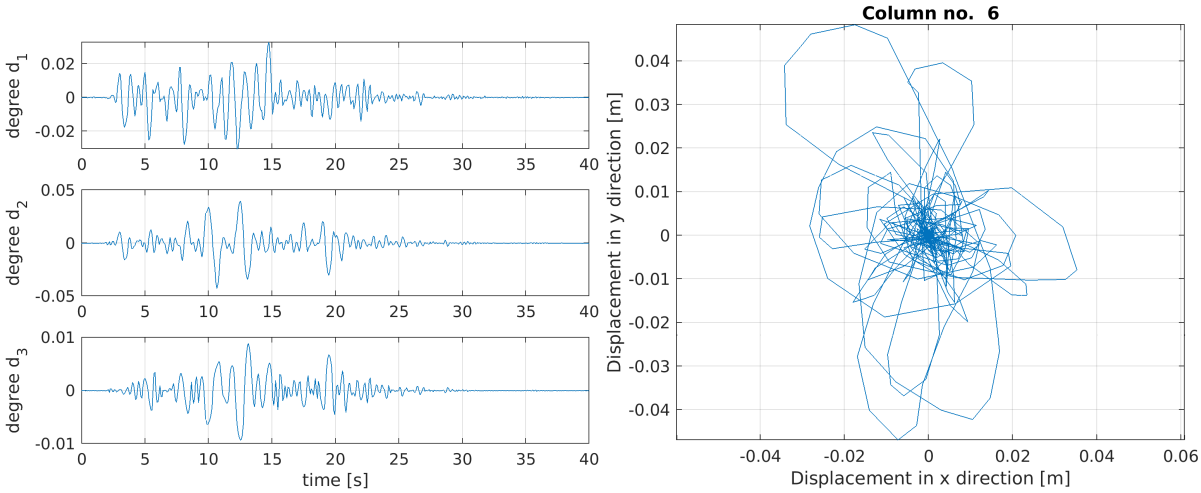

Figure 10: on the left side, the time histories of the degrees of freedom of the pulpit obtained for an earthquake with $T_r = 2475$ years; on the right, the trajectory of the top section of column no. 6, which is subject to the highest displacement.

Even though the values of the degrees of freedom might not appear too pronounced, the situation changes when the displacement of each column is evaluated by means of equations 1; for column no. 6 a maximum top displacement of about $54\,\mathrm{mm}$ is calculated. This, in turn, causes very high pressures in the interface of the column, as it can be seen from figure 11.

6 CONCLUSIONS

A ®MatLab code to investigate the dynamic behavior of the marble pulpit by Giovanni Pisano in the church of S. Andrea, Pistoia (Italy) has been presented; several hypotheses were introduced to simplify the procedure, some of which will be released in future versions.

The pulpit is likely to exhibit rocking response under earthquakes of moderate intensity, but it seems that its overturning is difficult to occur even under severe earthquakes. This condition is nevertheless to be verified in further versions of the code, as the vertical accelerations might

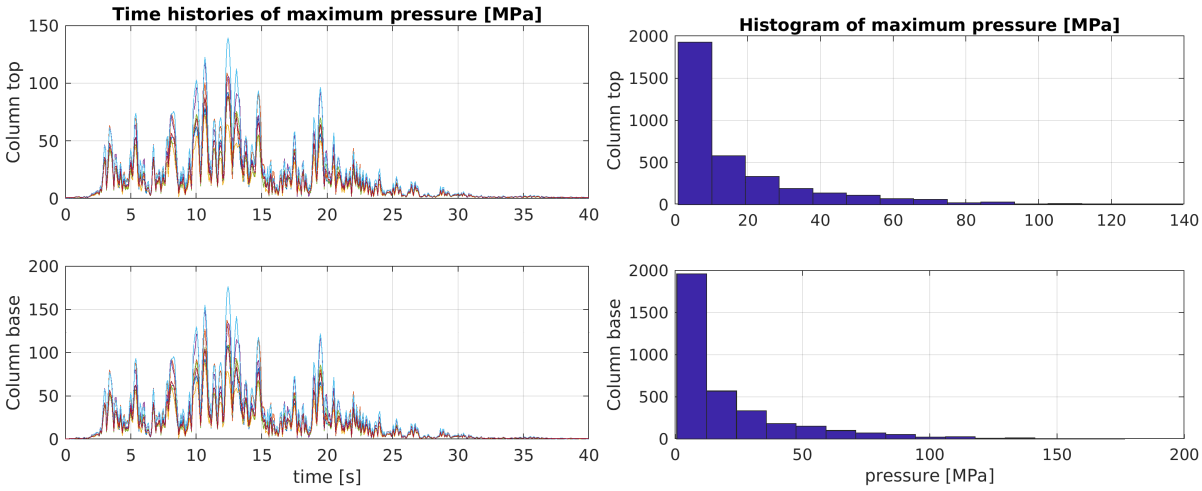

Figure 11: on the left, the time histories of the maximum pressures for each column is shown; on the right, the histogram of all the maximum pressures calculated in the interfaces of every column.

have great influence on the pulpit response.

Nevertheless, high pressure distributions are evaluated at the interfaces between the columns and their bases or the pulpit above, showing that a structural collapse due to material resistance is more likely to occur than the overturning condition.

REFERENCES

[1] G. Bartoli, M. Betti, V. Bonora, A. Conti, L. Fiorini, V. Cerisano Kovacevic, V. Tesi, G. Tucci, From TLS data to FE model: a workflow for studying the dynamic behavior of the Pulpit by Giovanni Pisano in Pistoia (Italy). *Procedia Structural Integrity*, **29**, 55–62, 2020.

[2] C. Blasi, P. Spinelli, A method to calculate the dynamics of systems made by superimposed rigid blocks (in Italian). *Ing. Sismica*, **1**, 12–21, 1986.

[3] L. Facchini, V. Gusella, P. Spinelli, Block random rocking and seismic vulnerability estimation. *Engineering Structures*, **16** (6), 412–424, 1994.